Original Article

Prediction of Molecular Interaction between Platelet Glycoprotein Ibα and von Willebrand Factor using Molecular Dynamics Simulations

Seiji Shiozaki[1], Shu Takagi[2] and Shinya Goto[1]

[1]Department of Medicine (Cardiology), Tokai University School of Medicine, Kanagawa, Japan
[2]Department of Mechanical Engineering, The University of Tokyo, Tokyo, Japan

***Aim*: The molecular mechanism of the unique interaction between platelet membrane glycoprotein Ibα (GPIbα) and von Willebrand Factor (VWF), necessary for platelet adhesion under high shear stress, is yet to be clarified.**
***Methods*: The molecular dynamics simulation using NAMD (Nanoscale Molecular Dynamics) package with the CHARMM 22 (Chemistry at Harvard Macromolecular Mechanics) force field were used to predict dynamic structural changes occurring in the binding site of A1 domain of VWF and N terminus domain of GPIbα under water soluble condition.**
***Results*: The mean distance between the mass center of A1 domain of VWF and GPIbα in the stable form was predicted as 27.3 Å. The potential of mean force between the A1 domain of VWF and GPIbα were calculated in conditions of various distances of the mass center between them. All the calculated values were fitted to the Morse potential energy function curve. The maximum adhesive force between A1 domain of VWF and GPIbα was predicted as 62.3 pN by differentiating the potential of mean force with respect to the molecular distance.**
***Conclusions*: The molecular dynamics simulation is useful for predicting the dynamic structure changes of protein bonds involved in platelet adhesion and for predicting the adhesive forces generated between their interactions.**

J Atheroscler Thromb, 2016; 23: 455-464.

Key words: von Willebrand factor, Glycoprotein Ib, Platelet shear, Flow

Introduction

In the initial stage of thrombus formation, platelet adhesion at site of endothelial injury plays a crucial role[1, 2]. Various *in vivo* and *in vitro* experiments demonstrated that glycoprotein Ibα (GPIbα), which is present on the platelet surface, and its interaction with von Willebrand factor (VWF), which is exposed at the site of endothelial injury, play an important role, especially under the flow conditions generating high wall shear stress[3-5]. Although there are other adhesive proteins such as glycoprotein IIb/IIIa (GPIIb/IIIa) to bind with VWF upon platelet activation[4-8], GPIbα binding with VWF is necessary for capturing flowing platelet to the vessel wall even when platelet cells were fully activated[5, 9].

Our previously published lattice model of the interaction between GPIbα and VWF for kinetic Monte Carlo method predicted that the number of the bonds between GPIbα and VWF should not exceed 100 due to space limitation[10]. Large and concentrated multimeric structure of VWF molecules is one potential characteristic to explain specific adhesive function between GPIbα and VWF[11]. Recent research progress showed the important regulatory functions of a disintegrin and metalloproteinase with a thrombospondin type 1 motif (ADAMTS)-13 for cleaving VWF multimer[12, 13]. Specific biomechanical characteristic of the

Address for correspondence: Shinya Goto, Department of Medicine (Cardiology), Tokai University School of Medicine, 143 Shimokasuya, Isehara, Kanagawa 259-1143, Japan
E-mail: shinichi@is.icc.u-tokai.ac.jp
Received: August 4, 2015
Accepted for publication: September 14, 2015

binding GPIbα and VWF was also reported in domain level using atomic force microscope[14, 15].

Here, we conducted a Molecular Dynamic simulation of the interaction between A1 domain of VWF and GPIbα. We have predicted the structure of A1 domain of VWF bound with GPIbα dissolved in water. We have predicted that the part of A1 domain (SER^{562}-ILE^{566} and ILE^{546}-TRP^{550}) remained bound with GPIbα just before dissociation. Unlike previous publications[16, 17], we have calculated the potential of mean force between A1 domain of VWF and GPIbα and predicted the adhesive force to be 62.3 pN. We have shown the usefulness of Molecular Dynamic simulation for understanding the molecular mechanism of platelet membrane protein interaction with vessels.

Methods

Molecular Dynamics

The interaction between N-terminal leucine rich repeat within GPIbα (residues HSE^{1}-PRO^{265}) molecule and A1 domain of VWF (residues ASP^{506}-PRO^{703}) was targeted in our study using Molecular Dynamics (MD) method[18]. The molecular dynamics simulation method is based on the Newton's second law; $F = ma$, where F is the force exerted on the atom and m and a are its mass and acceleration, respectively. Using the potential energy model taking into account of the coulombic interaction, the van der waals interaction and the hydrogen bonding, the force affecting each atom constructing both proteins and water can be calculated. Based on the value of the forces calculated from potential energy model, the acceleration of each atom can also be calculated. Integration of the equation of motion then yields a trajectory that describes the positions and velocities of the atoms as they vary with time. In our MD simulation, the initial structure of A1 domain of VWF bound with GPIbα was taken from the crystal structure[19]. It is noted that the structure we have referred to is an expansion of early publication[20] on a complex with R1306Q A1 domain of VWF and M239V GPIbα mutations, but the structure of the mutant are supposed to be close to their wild type. All MD simulations were conducted using the NAMD (Nanoscale Molecular Dynamics) package[21] with the CHARMM22 (Chemistry at Harvard Macromolecular Mechanics) force field[22], which refers to the form and parameters of the functions used to describe the potential energy of a system of atoms, in the canonical (NVT) ensemble, using a constant number of atoms (N), constant volume (V), and constant temperature (T). The system was solvated with the TIP3P (transferable intermolecular potential with three interaction sites) water molecules using VMD (Visual Molecular Dynamics)[23]. A time step of 2.0 femto-seconds was used. Particle Mesh Ewald (PME) summation[24] was used for the long-range electrostatic interactions, with a cut off length of 12 Å for the direct interactions. The estimation of the positions of proton, solvation of the system with water molecules, calculations of root mean square deviation (RMSD) and drawing of protein structures were done with VMD. The total number of atoms including the protein molecules and water molecules was about 172,934 in this system, whose size was $83 \times 95 \times 105$ Å with the periodic boundary conditions. Before starting the calculation to predict the equilibrated structure of the A1 domain of VWF bound with the N-terminus of GPIbα, our systems were initially energy-minimized with 10,000 steps of calculation. Our systems were equilibrated for 1 nano-second under constant temperature of 310 K controlled by Langevin dynamics[25] with a temperature coefficient of 5 ps^{-1}.

Potential of Mean Force between A1 Domain of VWF and GPIbα

In order to calculate the free energy profiles for the process of A1 domain of VWF binding with GPIbα, Potential of Mean Force (PMF) calculations were conducted using umbrella sampling method[26]. Each windows were separated by 0.5 Å, covering the reaction coordinate, which represent the distance between the center of mass of A1 domain of VWF and GPIbα N-terminal domain, from 20 to 78 Å. The total number of windows for each complex structure was 101. For each window, the MD simulations were performed for 10 nano-seconds at 310 K controlled by Langevin dynamics. The biasing force constant applied in the different windows of the umbrella sampling was 1.0 kcal/(mol·$Å^2$). The systems were first equilibrated for 2 nano-seconds and then kept for 10 nano-seconds to take a sample for a window. It took about 280 hours to complete 12 nano-seconds calculation on RICC (RIKEN Integrated Cluster of Clusters) facility with 32 processors. From the trajectory of 101 windows, the PMF was calculated using the weighted histogram analysis method (WHAM)[27]. The Morse potential, which is expressed as follows, was fitted to the obtained free energy profile using the Levenberg-Marquardt algorithm enabling to minimize the sum of integrated amount of deviation of each calculated value and the fitted curve[28].

$$U_M = D_e\{(1 - \exp(-a(r - r_e)))^2 - 1\} \quad (1)$$

Where r is the reaction coordinate (the distance between the center of mass of VWF and GPIbα), r_e is

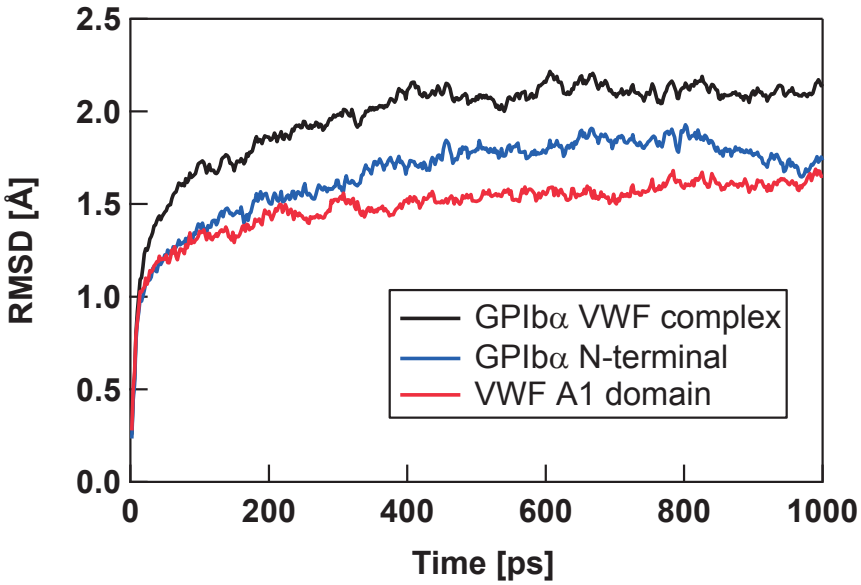

Fig. 1. Confirmation of Convergence in Our Molecular Dynamic Simulation Calculation.

The root mean square deviation (RMSD) of all atoms which constitute the A1 domain of VWF and N-terminus domain of GPIbα (black line), the A1 domain of VWF (red line) and N-terminus domain of GPIbα (blue line) starting from crystal structure (time 0) to 1000 pico-second is shown. The RMSD become convergent after 400 pico-seconds of calculation.

the reaction coordinate at equilibrium state, D_e is the well depth, and a controls the width of the potential.

Assuming that the proteins do not interact with each other when the distance between the mass centers of them exceeded certain value, the average PMF at that distance (r) was set to zero. By differentiating the Morse potential curve with respect to r, the mean (ensemble-averaged) force between GPIbα and VWF was calculated as predicted binding force between A1 domain of VWF and GPIbα. In order to evaluate the fitting error, the high accuracy fitting was conducted using the quartic function expressed as equation (2) around the r with highest binding force.

$$U_q = K_0 + K_1 r + K_2 r^2 + K_3 r^3 + K_4 r^4 \quad (2)$$

Where U_q is the Potential of Mean Force and K_0-K_4 are the fitting parameter.

Results

Equilibration of Our Calculation Model

As shown in **Fig. 1**, the root mean square deviation (RMSD) of all protein atoms, started with the crystal structure, changed after exposure to water and reached the equilibrated state after 400 pico-seconds of calculation (**Fig. 1**). The RMSD starting from crystal structure to the structure stable in the water was approximately 2.3 Å. The most stable water dissolved structure of VWF bound with GPIbα is shown in **Fig. 2** (dynamic change in the structure is shown in supplemental movie provided journal web site). The distance between the center of mass of VWF A1 domain and that of GPIbα N-terminal in this structure was 27.3 Å.

Potential of Mean Force between GPIbα and VWF Interactions

Each of red dots in **Fig. 3** shows the free energy (kcal/mol) calculated when the distance between mass center of VWF (A1 domain) and GPIbα (r) was settled at the value from 21 Å to 78 Å shown in the bottom of the figure. The maximum binding free energy for GPIbα bound with A1 domain of VWF in this stable structure was calculated to be −13.5 kcal/mol with the assumption that the proteins do not interact with each other when r value exceeded 50 Å. By fitting the Morse potential function to the PMF, the values of each parameter in equation (1) were determined as follows, D_e=13.5 kcal/mol, a=0.139, and r_e=27.3 Å. The Morse potential fitting curve is shown in red line in **Fig. 3**. The predicted binding force between A1 domain of VWF and GPIbα in respect to r is shown

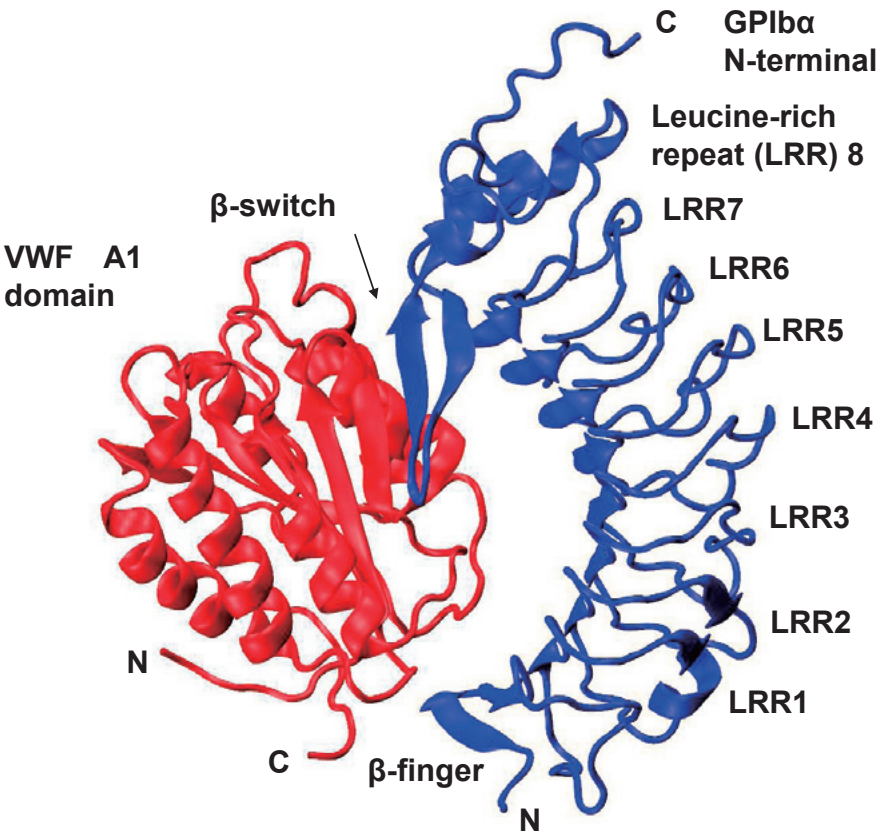

Fig. 2. Predicted Water-Soluble Molecular Structure of A1 domain of VWF bound with GPIbα.

Ribbon representation of the complex of VWF A1 domain and GPIbα. The VWF binding site of GPIbα is colored blue, and the VWF A1 domain is red. α-Helices are shown as coiled ribbons, β-stands as ribbons with arrows, and loops as tubes.

as blue line in **Fig. 3**. The predicted binding force become maximum to be 65.2 pN at the distance of 32.3 Å. The high accuracy fitting using equation (2) was applied from r-value of 27 Å to 37 Å (fitting parameters used were the followings; $K_0 = 1.41 \times 10^3$ kcal/mol, $K_1 = -1.74 \times 10^2$ kcal/(mol·Å), $K_2 = 7.83$ kcal/(mol·Å^2), $K_3 = -1.57 \times 10^{-1}$ kcal/(mol·Å^3) and $K_4 = 1.17 \times 10^{-3}$ kcal/(mol·Å^4)). Predicted maximum binding force of 62.3 pN was within 4.4% difference from that predicted from Morse potential fitting.

Fig. 4 (supplemental movie provided journal web site) shows the snapshots of the GPIbα-VWF complex with r value of 27.5, 31.0, 40.0 and 65.0 Å, respectively. The GPIbα N-terminal and VWF A1 domain stably binds with each other at r value of 27.5 Å (**Fig. 4 (a)**). The globular A1 domain interacts with the concave face of GPIbα. The interaction surface comprises two distinct sites of tight interactions (**Fig. 4 (b) (c)**). The first contact site is the N-terminal β-finger (residues Cys^4-Cys^{17}), and the second is the β-switch region (residues Val^{227}-Ser^{241}) of GPIbα, which interacts with the central β-sheet of VWF A1 (residues SER^{562}-ILE^{566}). When the r value reached to 65 Å, the GPIbα and A1 domain of VWF apparently dissociated (**Fig. 4 (d)**).

Discussion

Interaction between VWF and GPIbα plays an essential role for platelet adhesion to the damaged endothelium under various blood flow condition as illustrated in **Fig. 5**[4, 5, 29]. This interaction has a special characteristic not shared by other adhesive interactions of various platelet membrane proteins with their ligands; e.g. activated GPIIb/IIIa binding with fibrinogen/VWF or collagen binding to GPIa/IIa, which generates the binding force enabling platelets to stay adhered against high shear force generated in arterial level[30]. Previous study confirmed strong binding force between VWF and GPIbα with the use of atomic

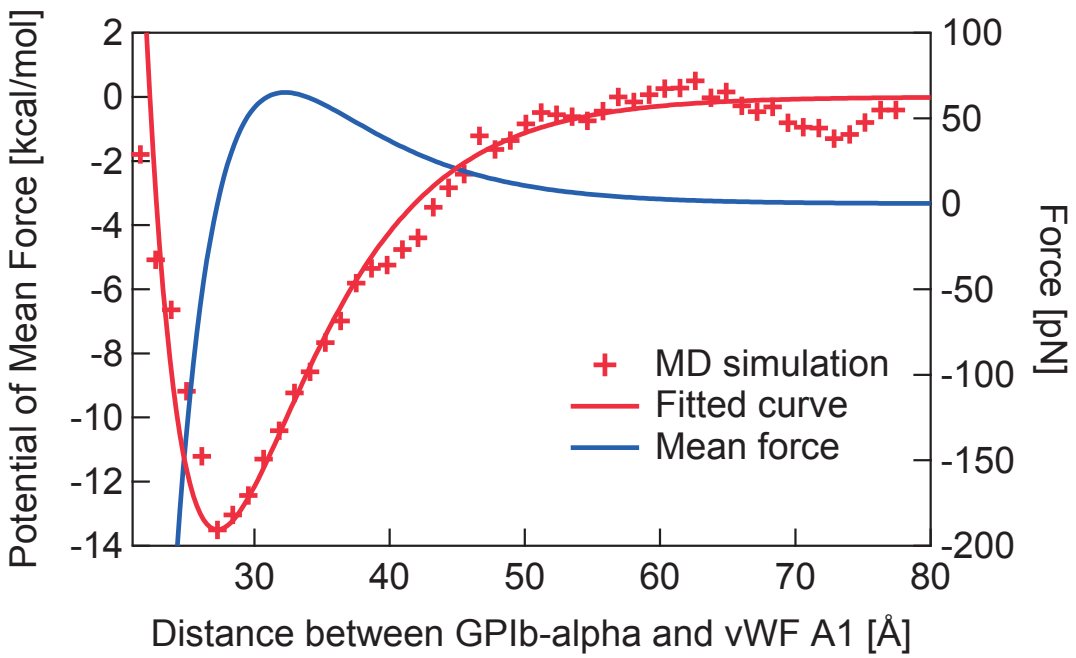

Fig. 3. Calculation of Potential of Mean Force, Morse Fitting and Force between A1 domain of VWF and GPIbα.

Potential of mean forces for binding between A1 domain of VWF and N-terminus domain of GPIbα (shown in Fig. 2) were calculated as kcal/mol in every 1 Å of the distance of the center of mass of both molecules as shown in red dots. The Morse potential curve was drawn to fit to all the calculated values to minimize the sum of integrated amount of deviation of each distance as shown in red line. The force curve was drawn by taking the diffrential of the fitted Morse potential curve in respect to the distance as shown in blue line.

force microscopy[14, 15]. Here, we have applied molecular dynamic computer simulation to the interaction between VWF and GPIbα. We have predicted the chemical structure of VWF A1 domain bound with N-terminus domain of GPIbα in soluble state with our simulation, which was similar to its crystalized structure[20]. We have confirmed the importance of specific sites within disulfide of A1 domain of VWF (SER^{562}-ILE^{566}) for the binding with the GPIbα in our molecular simulation. We have calculated the potential of mean force generated between GPIbα and VWF to predict adhesive force generated by their binding (62.3 pN), which was in agreement with the value predicted by biological experiments[15, 30]. The unbinding force, which is not exactly the same as the adhesive force, of a single bond between GPIbα and VWF was measured to be 54 pN using an atomic force microscope (AFM). In order to compare strictly the result of MD simulation with that of biological experiment, the unbinding rate should be modeled properly from the potential of mean force.

There are huge numbers of publications demonstrating the importance of A1 domain of VWF and leucine rich N-terminus domain of GPIbα for their specific biological interaction[30-38]. However, there are huge limitation in understanding the precise nature of VWF binding to GPIbα with the previously available biological methods. This was mostly because of the difficulty in reproducing the stable binding state without artificial conditions such as the presence of ristocetin[39] and/or botrocetin[40]. Of note, physiologically relevant binding of VWF to GPIbα, which generate the binding force strong enough to capture platelet under blood flow conditions, can be detected only transiently[4]. Moreover, the stable binding state detected in the presence of ristocetin (residues 702-704) was proven not to be relevant for binding under high shear stress condition[33, 39]. Accordingly, characterization of the chemical interaction between VWF and GPIbα is still to be elucidated by the currently available methodology[9].

Computer simulation is a new tool to understand the mechanism of biological phenomena. Several previous reports demonstrated that multiscale three-dimensional (3-D) numerical simulation is helpful for understanding the specific characteristic of platelet adhesion under various shear stress conditions[41, 42]. Indeed, transient binding of platelet on the

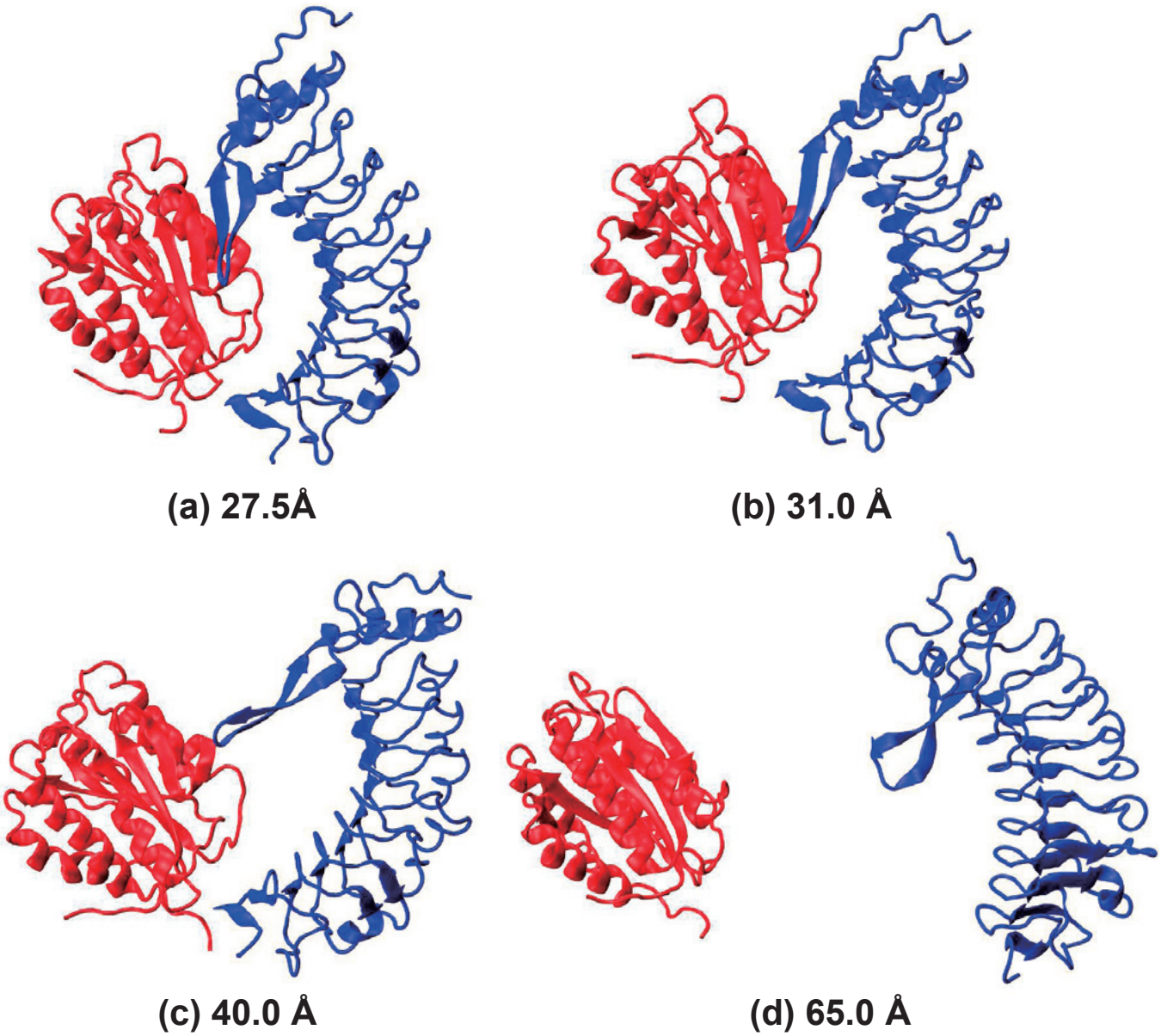

Fig. 4. Snapshots of A1 Domain of VWF bound with N-terminus domain of GPIbα at the Closest (27.5 Å) to the Dissociation (65.0 Å).

Snapshots of VWF/GPIbα complex along the reaction coordinate. The distance between the center of mass of GPIbα N-terminal and VWF A1 domain were constrained to 27.5, 31.0, 40.0, and 65.0 Å. The β-finger and the β-switch region of GPIbα interacted with VWF A1. The disulfide loop containing 185 amino acids in the A1 domain of VWF (residue 505-695) kept bound just before dissociation from GPIbα.

damaged endothelium, which is one of the specific characteristics of platelet interaction with VWF under high shear stress, was reproduced by their simulation[42]. The continuum models[43, 44], discrete element models[45, 46] and immersed-boundary methods[47] were shown to be applicable to reproduce platelet adhesion on the vessel wall. However, even with these new methodologies, specific characteristics of A1 domain of VWF binding with platelet GPIbα were not clarified in the molecular level. We have applied newly developed molecular dynamics simulation for VWF binding with GPIbα and predicted dynamic binding structure along with potential of mean force generated in this bond, which gave us further perspective in the understanding of these molecular interaction.

Molecular dynamic simulation technologies have

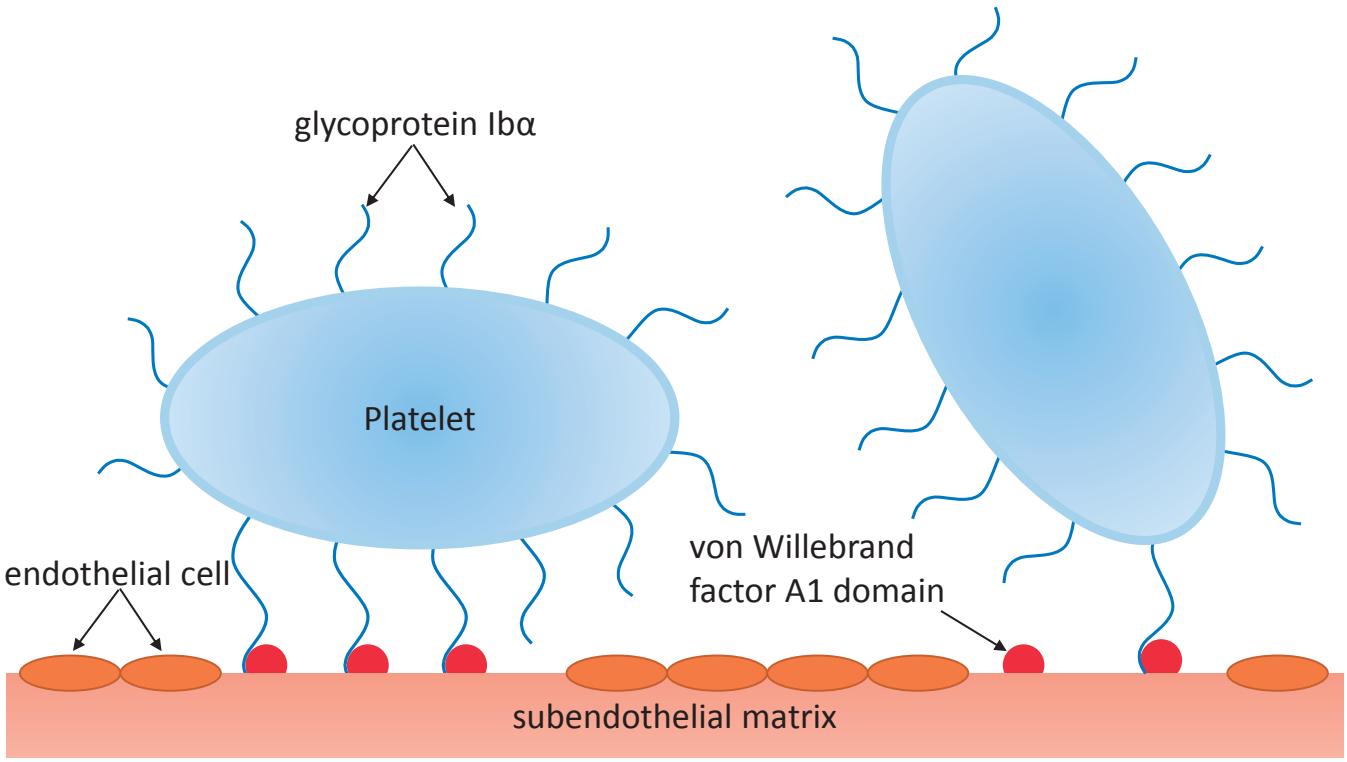

Fig. 5. Schematic illustration of platelet adhesion.

The membrane glycoprotein Ibα can initiate platelet adhesion to the immobilized A1 domain of von Willebrand factor while opposing elevated shear forces.

already been applied for detailed understanding of the mechanisms of various enzymes[48-51]. We have applied the established calculation software named NAMD package[52] with the CHARMM 22[53-56] for simulating molecular interaction between A1 domain of VWF and N-terminus domain of GPIbα. By Monte-Carlo simulation, we have previously shown that the localization GPIbα is a key determinant factor for platelet binding with large size of VWF molecule[57]. Adhesive force shall not exceed 300 pN due to space limitation caused by large molecular size of VWF[57]. Our calculation results demonstrate the maximum mean force of VWF binding to GPIbα to the value equivalent in platelet adhesion on damaged endothelium in arterial level that is mediated by less than 10 molecular bonds.

There are obvious methodological limitations in our method to apply our results in understanding complex biological phenomena. First, we have calculated the force generated between VWF and GPIbα by differentiating Morse potentials obtained by each calculated potential of mean forces with various distance between A1 domain of VWF and GPIbα. We have calculated molecular dynamics for Morse potential fitting. However, there is a potential risk of fitting error. The impact of fitting error might be substantially large. The maximum mean force value we predicted in our simulation of 62.3 pN is not against biological experiments, however, further quantitative comparison in the future is awaited. This is the first application of molecular dynamic simulation for prediction of force between VWF and GPIbα. Application of the same method for prediction of VWF and GPIbα interaction with mutant molecules and the other platelet membrane protein interaction with ligands are on going.

In conclusion, the equilibrium water soluble structure of A1 domain of VWF bound with GPIbα was determined with Molecular Dynamic calculation. The specific site within A1 domain loop (SER^{562}-ILE^{566}) was shown to act as the lasting binding site for GPIbα. The potential of mean force of the interaction between A1 domain of VWF and GPIbα was calculated using umbrella sampling method. From the potential of mean force, the maximum mean force between GPIbα and VWF A1 domain was estimated to be 62.3 pN. The function form of the potential was also obtained by fitting the curve to Morse Potential type.

Acknowledgements

We gratefully acknowledge T. Hasebe, S. Ii, K. Ishikawa, Y. Nanazawa, S. Noda, H. Oka, N. Shimamoto, K. Shimizu, K. Sugiyama, Y. Sunaga, N. Tamura, H. Yokota, and N. Miyashita for their helpful discussions during group meetings for thrombosis simulator development. The calculations were performed by using the RIKEN Integrated Cluster of Clusters (RICC) facility and K computer. This study was supported by the strategic programs for innovative research field 1 "Supercomputational Life Science" of the Ministry of Education, Culture, Sports, Science, and Technology (MEXT) of Japan. We acknowledge the correction of English Grammar by Dr. Shinichi Goto.

Funding

The author acknowledges financial support provided by a Grant-in-Aid for Scientific Research in Japan (24390202), a grant for the next-generation supercomputer Research and Development program supported by RIKEN, a grant from SENSHIN Medica Research Foundation and Strategic Program for Innovational Research Field 1 for Super-computational Life Science.

Conflicts of Interest

The author Shinya Goto received consulting fees and honoraria from Sanofi, Bayer HealthCare, AstraZeneca, Astellas, and Armethron. The author also received research grants from Sanofi and Pfeizer. Dr. Takagi and Dr. Shiozaki have no COI to disclose.

Reference

1) Kawamura Y, Takahari Y, Tamura N, Eguchi Y, Urano T, Ishida H and Goto S. Imaging of structural changes in endothelial cells and thrombus formation at the site of FeCl(3)-induced injuries in mice cremasteric arteries. J Atheroscler Thromb. 2009; 16: 807-814
2) Andre P, Denis CV, Ware J, Saffaripour S, Hynes RO, Ruggeri ZM and Wagner DD. Platelets adhere to and translocate on von Willebrand factor presented by endothelium in stimulated veins. Blood. 2000; 96: 3322-3328
3) McGhie AI, McNatt J, Ezov N, Cui K, Mower LK, Hagay Y, Buja LM, Garfinkel LI, Gorecki M and Willerson JT. Abolition of cyclic flow variations in stenosed, endothelium-injured coronary arteries in nonhuman primates with a peptide fragment (VCL) derived from human plasma von Willebrand factor-glycoprotein Ib binding domain. Circulation. 1994; 90: 2976-2981
4) Savage B, Saldivar E and Ruggeri ZM. Initiation of platelet adhesion by arrest onto fibrinogen or translocation on von Willebrand factor. Cell. 1996; 84: 289-297
5) Goto S, Ikeda Y, Saldivar E and Ruggeri ZM. Distinct mechanisms of platelet aggregation as a consequence of different shearing flow conditions. J Clin Invest. 1998; 101: 479-486
6) Shattil SJ, Motulsky HJ, Insel PA, Flaherty L and Brass LF. Expression of fibrinogen receptors during activation and subsequent desensitization of human platelets by epinephrine. Blood. 1986; 68: 1224-1231
7) Niiya K, Hodson E, Bader R, Byers-Ward V, Koziol JA, Plow EF and Ruggeri ZM. Increased surface expression of the membrane glycoprotein IIb/IIIa complex induced by platelet activation. Relationship to the binding of fibrinogen and platelet aggregation. Blood. 1987; 70: 475-483
8) Michelson AD and Barnard MR. Thrombin-induced changes in platelet membrane glycoproteins Ib, IX, and IIb-IIIa complex. Blood. 1987; 70: 1673-1678
9) Goto S, Salomon DR, Ikeda Y and Ruggeri ZM. Characterization of the unique mechanism mediating the shear-dependent binding of soluble von Willebrand factor to platelets. J Biol Chem. 1995; 270: 23352-23361
10) Shiozaki S, Ishikawa, KL, Takagi, S. Numerical study on platelet adhesion to vessel walls using the kinetic monte carlo method. J Biomech Sci Eng. 2011; 7: 275-293
11) Moake JL, Rudy CK, Troll JH, Weinstein MJ, Colannino NM, Azocar J, Seder RH, Hong SL and Deykin D. Unusually large plasma factor VIII: von Willebrand factor multimers in chronic relapsing thrombotic thrombocytopenic purpura. N Engl J Med. 1982; 307: 1432-1435
12) Banno F, Kaminaka K, Soejima K, Kokame K and Miyata T. Identification of strain-specific variants of mouse Adamts13 gene encoding von Willebrand factor-cleaving protease. J Biol Chem. 2004; 279: 30896-30903
13) Furlan M, Robles R, Galbusera M, Remuzzi G, Kyrle PA, Brenner B, Krause M, Scharrer I, Aumann V, Mittler U, Solenthaler M and Lammle B. von Willebrand factor-cleaving protease in thrombotic thrombocytopenic purpura and the hemolytic-uremic syndrome. N Engl J Med. 1998; 339: 1578-1584
14) Kim J, Zhang CZ, Zhang X and Springer TA. A mechanically stabilized receptor-ligand flex-bond important in the vasculature. Nature. 2010; 466: 992-995
15) Tobimatsu H, Nishibuchi Y, Sudo R, Goto S and Tanishita K. Adhesive Forces between A1 Domain of von Willebrand Factor and N-terminus Domain of Glycoprotein Ibalpha Measured by Atomic Force Microscopy. J Atheroscler Thromb. 2015; 22: 1091-1099
16) Liu G, Fang Y and Wu J. A mechanism for localized dynamics-driven affinity regulation of the binding of von Willebrand factor to platelet glycoprotein Ibalpha. J Biol Chem. 2013; 288: 26658-26667
17) Li J, Zhang L and Sun Y. Molecular basis of the initial platelet adhesion in arterial thrombosis: molecular dynamics simulations. Journal of molecular graphics & modelling. 2012; 37: 49-58
18) Doucet J and Benoit JP. Molecular dynamics studied by analysis of the X-ray diffuse scattering from lysozyme crystals. Nature. 1987; 325: 643-646
19) Dumas JJ, Kumar R, McDonagh T, Sullivan F, Stahl ML,

Somers WS and Mosyak L. Crystal structure of the wild-type von Willebrand factor A1-glycoprotein Ibalpha complex reveals conformation differences with a complex bearing von Willebrand disease mutations. J Biol Chem. 2004; 279: 23327-23334
20) Huizinga EG, Tsuji S, Romijn RA, Schiphorst ME, de Groot PG, Sixma JJ and Gros P. Structures of glycoprotein Ibalpha and its complex with von Willebrand factor A1 domain. Science. 2002; 297: 1176-1179
21) Phillips JC, Braun R, Wang W, Gumbart J, Tajkhorshid E, Villa E, Chipot C, Skeel RD, Kale L and Schulten K. Scalable molecular dynamics with NAMD. J Comput Chem. 2005; 26: 1781-1802
22) MacKerell AD, Jr., Banavali N and Foloppe N. Development and current status of the CHARMM force field for nucleic acids. Biopolymers. 2000; 56: 257-265
23) Humphrey W, Dalke A and Schulten K. VMD: visual molecular dynamics. J Mol Graph. 1996; 14: 33-38, 27-28
24) Abraham MJ and Gready JE. Optimization of parameters for molecular dynamics simulation using smooth particle-mesh Ewald in GROMACS 4.5. J Compt Chem. 2011; 32: 2031-2040
25) Grest GS and Kremer K. Molecular dynamics simulation for polymers in the presence of a heat bath. Phys Rev A. 1986; 33: 3628-3631
26) Rajamani R, Naidoo KJ and Gao J. Implementation of an adaptive umbrella sampling method for the calculation of multidimensional potential of mean force of chemical reactions in solution. J Compt Chem. 2003; 24: 1775-1781
27) Kumar S, Rosenberg JM, Bouzida D, Swendsen RH and Kollman PA. Multidimensional Free-Energy Calculations Using the Weighted Histogram Analysis Method. J Compt Chem. 1995; 16: 1339-1350
28) Lera G and Pinzolas M. Neighborhood based Levenberg-Marquardt algorithm for neural network training. IEEE transactions on neural networks / a publication of the IEEE Neural Networks Council. 2002; 13: 1200-1203
29) Nieswandt B, Brakebusch C, Bergmeier W, Schulte V, Bouvard D, Mokhtari-Nejad R, Lindhout T, Heemskerk JW, Zirngibl H and Fassler R. Glycoprotein VI but not alpha2beta1 integrin is essential for platelet interaction with collagen. EMBO J. 2001; 20: 2120-2130
30) Ruggeri ZM, Orje JN, Habermann R, Federici AB and Reininger AJ. Activation-independent platelet adhesion and aggregation under elevated shear stress. Blood. 2006; 108: 1903-1910
31) Celikel R, Varughese KI, Madhusudan, Yoshioka A, Ware J and Ruggeri ZM. Crystal structure of the von Willebrand factor A1 domain in complex with the function blocking NMC-4 Fab. Nat Struct Biol. 1998; 5: 189-194
32) De Marco L, Mazzuccato M, Grazia Del Ben M, Budde U, Federici AB, Girolami A and Ruggeri ZM. Type IIB von Willebrand factor with normal sialic acid content induces platelet aggregation in the absence of ristocetin. Role of platelet activation, fibrinogen, and two distinct membrane receptors. J Clin Invest. 1987; 80: 475-482
33) Miyata S and Ruggeri ZM. Distinct structural attributes regulating von Willebrand factor A1 domain interaction with platelet glycoprotein Ibalpha under flow. J Biol Chem. 1999; 274: 6586-6593
34) Murata M, Russell SR, Ruggeri ZM and Ware J. Expression of the phenotypic abnormality of platelet-type von Willebrand disease in a recombinant glycoprotein Ib alpha fragment. J Clin Invest. 1993; 91: 2133-2137
35) Murata M, Ware J and Ruggeri ZM. Site-directed mutagenesis of a soluble recombinant fragment of platelet glycoprotein Ib alpha demonstrating negatively charged residues involved in von Willebrand factor binding. J Biol Chem. 1991; 266: 15474-15480
36) Sugimoto M, Mohri H, McClintock RA and Ruggeri ZM. Identification of discontinuous von Willebrand factor sequences involved in complex formation with botrocetin. A model for the regulation of von Willebrand factor binding to platelet glycoprotein Ib. J Biol Chem. 1991; 266: 18172-18178
37) Weiss HJ, Hoffmann T, Yoshioka A and Ruggeri ZM. Evidence that the arg1744 gly1745 asp1746 sequence in the GPIIb-IIIa-binding domain of von Willebrand factor is involved in platelet adhesion and thrombus formation on subendothelium. J Lab Clin Med. 1993; 122: 324-332
38) Goto S, Ikeda Y, Murata M, Handa M, Takahashi E, Yoshioka A, Fujimura Y, Fukuyama M, Handa S and Ogawa S. Epinephrine augments von Willebrand factor-dependent shear-induced platelet aggregation. Circulation. 1992; 86: 1859-1863
39) Azuma H, Sugimoto M, Ruggeri ZM and Ware J. A role for von Willebrand factor proline residues 702-704 in ristocetin-mediated binding to platelet glycoprotein Ib. Thromb Haemost. 1993; 69: 192-196
40) Girma JP, Takahashi Y, Yoshioka A, Diaz J and Meyer D. Ristocetin and botrocetin involve two distinct domains of von Willebrand factor for binding to platelet membrane glycoprotein Ib. Thromb Haemost. 1990; 64: 326-332
41) Mody NA and King MR. Platelet adhesive dynamics. Part I: characterization of platelet hydrodynamic collisions and wall effects. Biophys J. 2008; 95: 2539-2555
42) Mody NA and King MR. Platelet adhesive dynamics. Part II: high shear-induced transient aggregation via GPIbalpha-vWF-GPIbalpha bridging. Biophys J. 2008; 95: 2556-2574
43) Fogelson AL and Guy RD. Platelet-wall interactions in continuum models of platelet thrombosis: formulation and numerical solution. Math Med Biol. 2004; 21: 293-334
44) Fogelson AL, Hussain YH and Leiderman K. Blood clot formation under flow: the importance of factor XI depends strongly on platelet count. Biophys J. 2012; 102: 10-18
45) Miyazaki H and Yamaguchi T. Formation and destruction of primary thrombi under the influence of blood flow and von Willebrand factor analyzed by a discrete element method. Biorheology. 2003; 40: 265-272
46) Tomita A, Tamura, N. Nanazawa, Y, Shiozaki, S. and Goto, S. Development of Virtual Platelet Implementing the Function of Three Platelet Membrane Proteins with Different Adhesive Characteristics. J Atheroscler Thromb. 2015; 22: 201-210
47) Fogelson AL and Guy RD. Immersed-boundary-type

models of intravascular platelet aggregation. Comput Method Appl M. 2008; 197: 2087-2104
48) Northrup SH, Pear MR, McCammon JA and Karplus M. Molecular dynamics of ferrocytochrome c. Nature. 1980; 286: 304-305
49) Levitt M. Molecular dynamics of hydrogen bonds in bovine pancreatic trypsin inhibitor protein. Nature. 1981; 294: 379-380
50) Oelschlaeger P, Klahn M, Beard WA, Wilson SH and Warshel A. Magnesium-cationic dummy atom molecules enhance representation of DNA polymerase beta in molecular dynamics simulations: improved accuracy in studies of structural features and mutational effects. J Mol Biol. 2007; 366: 687-701
51) Warshel A. Molecular dynamics simulations of biological reactions. Acc Chem Res. 2002; 35: 385-395
52) Jiang W, Hardy DJ, Phillips JC, Mackerell AD, Jr., Schulten K and Roux B. High-performance scalable molecular dynamics simulations of a polarizable force field based on classical Drude oscillators in NAMD. J Phys Chem Lett. 2011; 2: 87-92
53) Hynninen AP and Crowley MF. New faster CHARMM molecular dynamics engine. J Comput Chem. 2014; 35: 406-413
54) Riahi S and Rowley CN. The CHARMM-TURBOMOLE interface for efficient and accurate QM/MM molecular dynamics, free energies, and excited state properties. J Comput Chem. 2014; 35: 2076-2086
55) Sarzynska J, Reblova K, Sponer J and Kulinski T. Conformational transitions of flanking purines in HIV-1 RNA dimerization initiation site kissing complexes studied by CHARMM explicit solvent molecular dynamics. Biopolymers. 2008; 89: 732-746
56) Sjoqvist J, Linares M, Lindgren M and Norman P. Molecular dynamics effects on luminescence properties of oligothiophene derivatives: a molecular mechanics-response theory study based on the CHARMM force field and density functional theory. Phys Chem Chem Phys. 2011; 13: 17532-17542
57) Shiozaki SI, K. Takagi, S. Numerical study on platelet adhesion to vessel walls using kinetic Monte Carlo Method. J Biomech Eng. 2012; 7: 275-283